17. Sympozjum Mikromaszyny i Serwonapędy MiS 2011

Stefan BROCK[1)]
Marcin KANAREK[2]

Energy-efficient Control Algorithms of Permanent Magnet Synchronous Motors for Fan Applications

The paper deals with the problem of V/f control of a Permanent Magnet Synchronous Motor without winding dumper for fan applications. Voltage optimization was carried out in order to minimize the input power of PMSM. A model of the motor, that takes into account core losses and copper losses, has been presented. The relation between rotor speed and both types of losses has been established. Gained knowledge has been used to propose energy-optimal vector control strategy. Simulation results confirmed the validity of the applied solution for fan applications.

1. Introduction

In the last decade, the use of permanent magnet synchronous motors (PMSM) in motion control applications has significantly increased due to their features such as high efficiency and high power density [1]. In servo applications, in order to achieve high dynamic performance in torque, speed and position response the field orientation should be applied in a closed loop control [2]-[3]. The PMSM control requires a position sensor such as an incremental or absolute encoder, which increases the cost and decreases the reliability of the control system. Therefore, PMSM sensorless control is widely used. Many papers have as their main focus to eliminate position sensors. One of the methods used is a sensorless vector control, which estimates the rotor position by using, for example, the motor's electromotive force [4], or by using a Kalman filter [5,6]. The second method is V/f control in an open loop without rotor position. In applications such as pumps and fans, where a high dynamic is not required, a simple V/f control method can be applied instead of field oriented control [7]-[10]. In many applications, interior-type PMSMs with dumping windings are used for open-loop V/f control. Consequently the system is stable. However due to high cost, PMSMs with dumping windings are not often used. PMSMs without dumping windings do not ensure synchronization between the rotor and stator to the control V/f. It is a cause of instability of the system of PMSMs in open loop V/f control. Therefore, additional signals are needed to ensure synchronization and stable operation in V/f control.

In [8]-[10], in order to achieve stability to control V/f with PMSM without dumper windings, a dc-link current feedback was used. In [7], a new method of V/f control with PMSM without dumping windings in the rotor is proposed. In this method, stator voltage is calculated in order to maintain constant stator flux. This allows working with constant torque in the full frequency range. To stabilize the system for the full frequency range, additional

[1)] dr inż., Poznan University of Technology, Institute of Control and Information Engineering, ul. Piotrowo 3A, 60-965 Poznań, tel. +(48-61)6652627, fax: +(48-61)6652365, e-mail: Stefan.Brock@put.poznan.pl

[2)] mgr inż., Poznan University of Technology, Institute of Control and Information Engineering, ul. Piotrowo 3A, 60-965 Poznań, tel. +(48-61)6652810, fax: +(48-61)6652365, e-mail: Marcin.Kanarek@put.poznan.pl

damping of the rotor is required. This can be achieved by an appropriate modulation of the frequency of the motor.

In [12, 13] an analysis of the stability of PMSM with fan load was carried out. Its results show that the PMSM without dumping windings is unstable. An additional stabilizing loop was introduced.

In this paper, an extensive simulation study for PMSM without windings dumper for open loop V/f control was carried out, where voltage is calculated in order to maintain a constant stator flux. Voltage optimization was carried out in order to minimize the input power of the PMSM. Simulation studies confirmed the validity of the applied solution. They are also a good starting point for future experimental studies.

2. PMSM model accounting for core and copper losses.

With the assumptions that spatial distributions of the magnetic flux in the air gap is sinusoidal and that the magnetic circuit is linear, the equations of the model are as follows [14]:

$$L_{Ld}\frac{di_d}{dt} = \left(v_d - Ri_d - L_{Mq}\frac{di_{od}}{dt} + L_q\omega i_{oq}\right) \tag{1}$$

$$L_{Lq}\frac{di_q}{dt} = \left(v_q - Ri_q - L_{Mq}\frac{di_{oq}}{dt} + L_d\omega i_{od} - \lambda_{PM}\right) \tag{2}$$

$$\omega = p\omega_r \tag{3}$$

$$i_{cd} - i_d - i_{cd} \tag{4}$$

$$i_{oq} = i_q - i_{cq} \tag{5}$$

$$i_{cd} - \frac{-\omega L_q i_{oq} + L_{Md}\frac{di_{od}}{dt}}{R_c} \tag{6}$$

$$i_{cq} - \frac{\omega(\lambda_{PM} + L_d i_{od}) + L_{Mq}\frac{di_{oq}}{dt}}{R_c} \tag{7}$$

$$T_e - \frac{3}{2}p\{\lambda_{PM} i_{oq} + (L_{Md} - L_{Mq}) i_{od} i_{oq}\} \tag{8}$$

$$i_{oq} - \left\{\frac{2T_e}{3p}\cdot\frac{1}{\lambda_{PM} + (L_{Md} - L_{Mq}) i_{od}}\right\} \tag{9}$$

$$J\frac{d\omega}{dt} = T_e - T_m \tag{10}$$

losses in steady state:

$$P_{Cu} = \frac{3}{2}R(i_d^2 + i_q^2) = \frac{3}{2}R\left\{\left(i_{od} \quad \frac{\omega L_q i_{oq}}{R_c}\right)^2 + \left(i_{oq} \quad \frac{\omega(\lambda_{PM} + L_d i_{od})}{R_c}\right)^2\right\} \tag{11}$$

$$P_{Fe} = \frac{3}{2}R_C(i_{cd}^2 + i_{cq}^2) = \frac{3\omega^2}{2R_C}\left\{(L_q i_{oq})^2 + (\lambda_{PM} + L_d i_{od})^2\right\} \tag{12}$$

where:

i_d, i_q – currents in direct and quadrature axes

i_{cd}, i_{cu} – currents in the core (d-q axes)

i_{od}, i_{oq} – stator currents (d-q axes)

v_d, v_q – voltages in d-q axes

L_d, L_{Md}, L_{Ld} – inductances in direct axis, consecutively – total, magnetizing, leakage

L_q, L_{Mq}, L_{Lq} – inductances In quadrature axis, consecutively – total, magnetizing, leakage

R , R_C – stator resistance and core (transversal) resistance (for 1 st harmonic)

λ_{PM} – permanent magnet flux

p – number of pole pairs

ω_R – mechanical speed

T_e, T_m – electrical and mechanical torque

P_{Cu}, P_{Fe} – copper and core losses in steady state

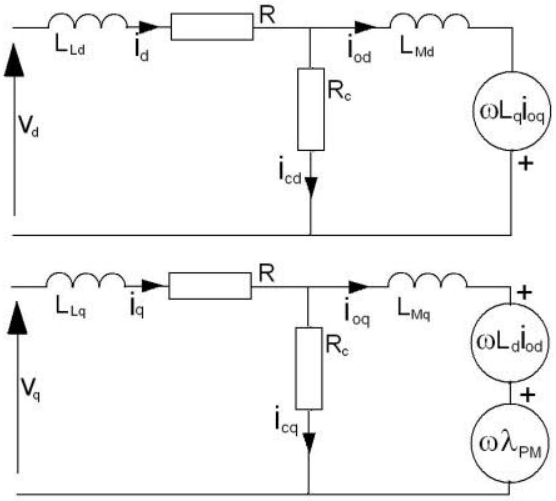

Fig. 1. Direct and quadratic axis equivalent circuits of PMSM

Both types of losses (core and copper) are function of speed and currents as shown in equations (12) and (13). Total electrical losses are sum of copper and core losses so they can too be shown as function of these three variables:

$$P_E = P_{Cu} + P_E = f(\omega, i_{od}, i_{oq}) \tag{13}$$

Due to relationships between variables (4), (6), (9) it is possible to formulate losses as functions of other variables, for example:

$$P_E = P_{Cu} + P_E = f_2(\omega, i_d, T_e) \tag{14}$$

Finally, in case of fan application, torque is function of speed and speed, in turn, is derived from pumped volume, so losses may be considered as function of two variables:

$$P_E - f_3(Q, i_d) \tag{15}$$

3. Fan and vent system model

Output of ventilated system increases with pressure, but this growth is nonlinear and generally slower than proportional. It is often assumed that volume is proportional to the square root of pressure. Literature on the subject often considers this relation (called flow characteristic) in reversed axes i.e. as $\Delta s = f(Q)$, where Q is volume and Δs is difference of pressures before and after fan. Note that usually notation Δp is used instead of Δs , but we already used p as number of pole pairs. In the figure 2 example was given.

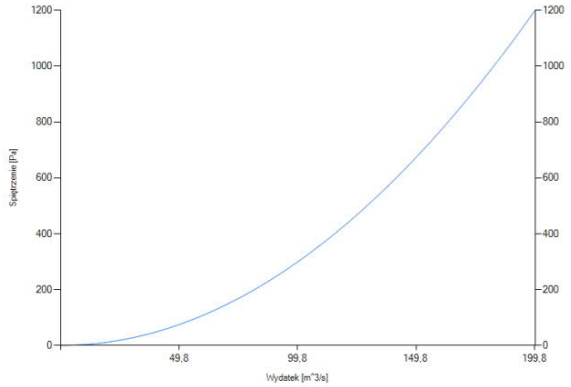

Fig. 2. Example of vent system flow characteristic

Fan flow characteristic, on the other hand, usually decreases with volume. Crossing point of fan and system characteristics sets working point of the whole structure. As power of the fan equals $P = \Delta s \cdot Q$, there exists working point, where power is maximal. It is important to fit fan type to the system so that working point would be close to this optimum [15].

PMSM usage allows for fluent speed control, so the fan characteristic may be adjusted thus allowing for fluent volume and pressure control. It is known that (approximately) volume is proportional to speed i.e. $Q = \frac{\omega}{\omega_N} \cdot Q_N$ and pressure is proportional to speed square $\Delta s = \left(\frac{\omega}{\omega_N}\right)^2 \Delta s_N$. Figure 3 shows fan characteristics for speeds ranging from 60% to 100% of nominal, related working points and power characteristic for motor working with full speed. At this case fan is well fit. Optimal working point (OP) exists at volume $Q = 132{,}7\ m^3/s$ and pressure $\Delta s - 3146 Pa$. This corresponds to power about 417,5 kW. Working point (WP) at that speed has coordinates $Q = 134{,}9\ m^3/s$ and $\Delta s = 3092\ Pa$. Horizontal distance between points on the figure exists because OP and power characteristic are drawn using the power scale (right hand).

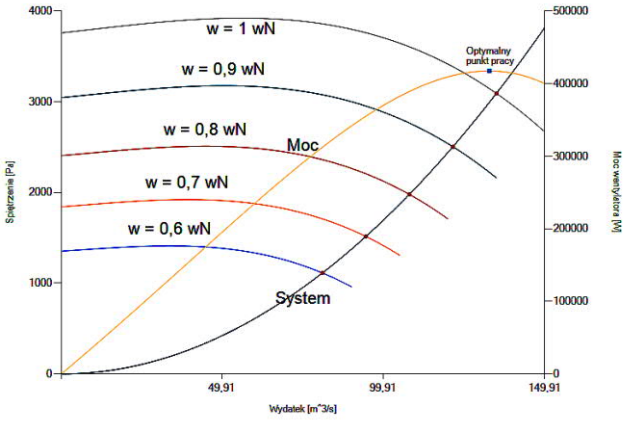

Fig. 3. Fan and system flow characteristics

Working motor is loaded with mechanical torque T_m:

$$T_m = \frac{Q \cdot s}{\eta_f \cdot \omega_r} + T_0 + \beta_f \cdot \frac{Q_N \cdot s_N}{\omega_{rN}} \cdot \left(\frac{\omega_r}{\omega_{rN}}\right)^q \tag{16}$$

where:

T_0 – static friction torque

β_f – dynamic friction coefficient

q – power coefficient on which determines how friction depends of speed. Experiments in this paper use value 1.2

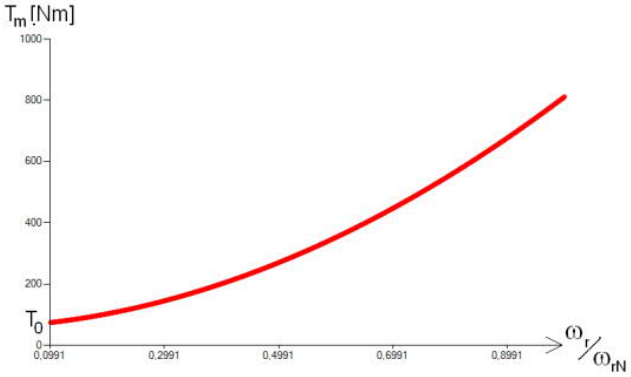

Fig. 4. Torque characteristic

4. Energy-efficient vector motor control

The following simulations (4.2, 4.3 and 4.4) has been performed with use of Matlab package and with help of self-made custom application. Experiment 1 purpose was to find optimal value of i_d current for motor working with chosen speed and torque. In experiment 2, optimal pair of values of speed and i_d was looked for with the assumption that motor generates constant power. Finally, in third experiment, optimal i_d for chosen volume was searched.

First two experiments used model of PMSM with following parameters:

$\lambda_{PM} = 0{,}0844[Wb]; p = 3; L_d = 9{,}77[mH]; L_{Md} = 7{,}33[mH]; L_q = 14{,}94\ [mH];$
$L_{Mq} = 11{,}21[mH]; R = 2{,}21[\Omega]; R_s = 840[\Omega]$

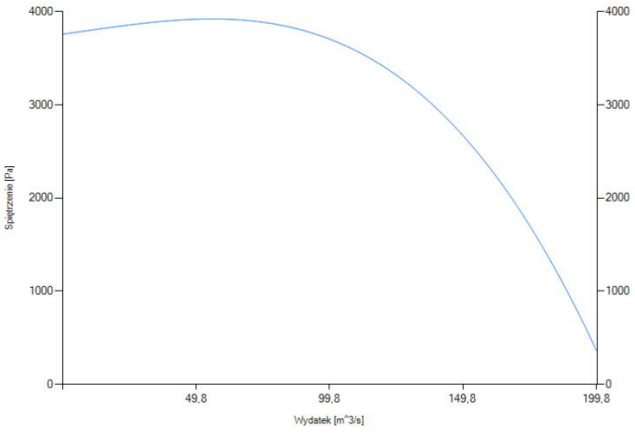

Fig. 5. Fan flow characteristic

Third experiment used different model of larger motor, derived from WDS380B6015 produced by Wuhan Directly-Driven Motor Co., Ltd. Its parameters are [16]:

$P_N - 200[kW];\ i_N - 376[A]; T_N - 1{,}27[kNm]; \omega_N - 157\left[\frac{rad}{s}\right]; \lambda_{PM} - 0{,}56[Wb];$

$p = 4; L_d = 9{,}77[mH]; L_{Md} = 7{,}33[mH]; L_q = 14{,}94\ [mH];\ L_{Mq} = 11{,}21[mH];$
$R = 0{,}05[\Omega];\ R_c = 840[\Omega]$

This experiment also used model of the fan [17], which flow characteristic was approximated by polynomial function $\Delta s = 3757{,}2 + 3{,}936Q + 0{,}0018Q^2 - 0{,}00059Q^3$ (shown at figure 5), vent system in this experiment had flow characteristic as $\Delta s = 0{,}17Q^2$.

4.1. Application

For purpose of research, dedicated utility application has been written in C# using Microsoft Visual Studio 2010. It uses .Net Framework 4.0 technology and MS Chart add-on.

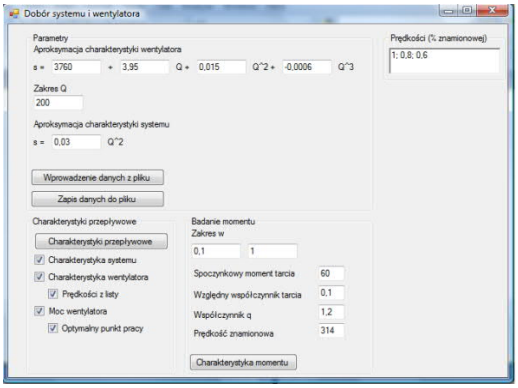

Fig. 6. Application main window

This application allows for:

- Entering data of fan and system characteristic from file, editing it and saving to file
- Computation and charting of flow characteristics $\Delta s = f(Q)$ for different speeds and mechanical characteristic $P - f(Q)$ as shown on figures 2 and 3.
- Computation of working points for these speeds (figure 3).
- Finding and charting load characteristic (figure 4)
- Auxiliary actions like saving charted characteristics to graphics files.

4.2. Experiment 1

For each instance of experiment, speed and torque was chosen. Then, range of current i_d, from $-4A$ to was quantized with step $0{,}01A$, resulting in set of 501 values. For each element of this set, responding value of i_{oq} was computed from equation 9. For each pair $\{i_{od}, i_{oq}\}$ core currents was computed from equations (6) and (7) and then total currents was obtained from set of fours $\{i_{od}, i_{oq}, i_{cd}, i_{cq}\}$. Then from equations (11) and (12) losses was computed resulting in characteristic $P = f(i_d)$ for each pair (ω, T_e). As seen on figure 7, in both cases optimal current i_{od} is negative. The i_d current, needed by controller, can be easily obtained from i_{od}. The optimal value of current decreases with torque increase as shown on figure 8.

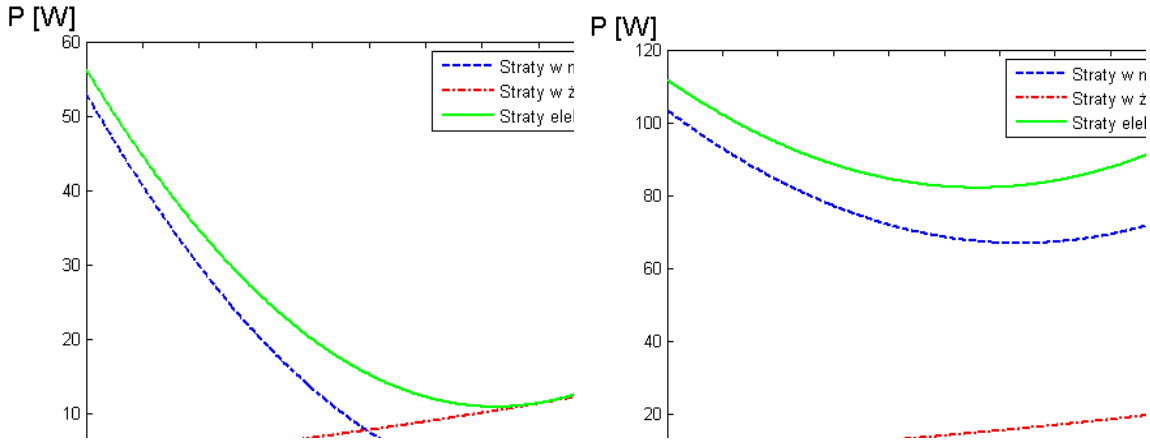

Fig. 7. Losses (copper, core and total) as function of i_{od} current. Speed equals and torque is (left side) and nominal ($1.7[Nm]$, right side)

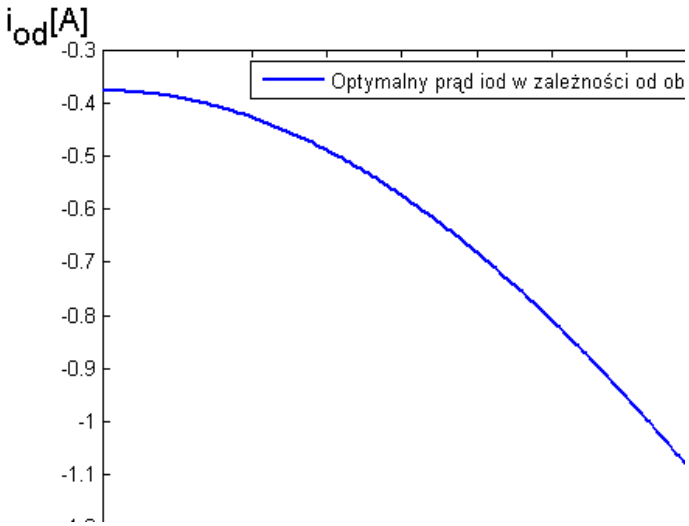

Fig. 8. Optimal current i_{od} as function of torque

4.3. Experiment 2

Second experiment is generalization of the first. For each element of set of speeds from range to , torque was chosen, such that motor power $P - \omega \cdot T_e$ equals its nominal power $540[W]$. Then, for each pair $\{\omega, T_e\}$, procedure from experiment 1 was repeated. The effect is surface plot of function of two variables. Its sections along speed axis would be functions similar to those from figure 7.

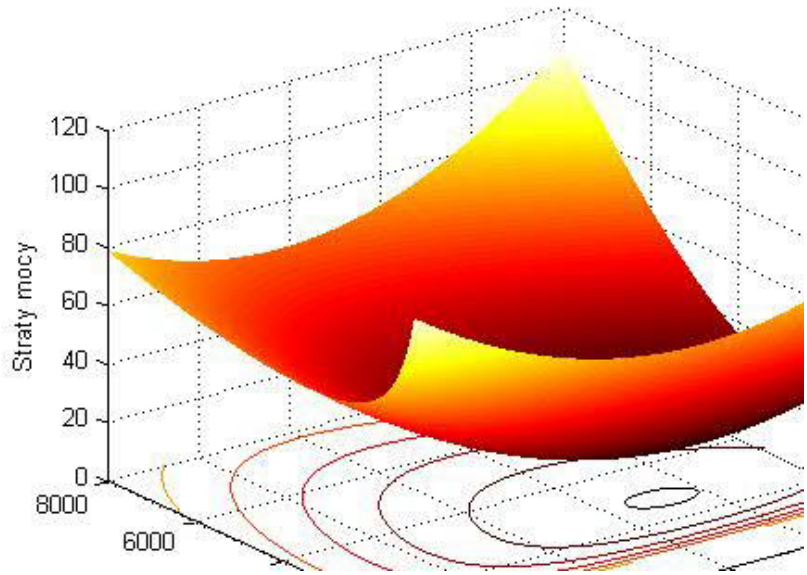

Fig. 9. Losses with mechanical power at 540 [W]

4.4. Experiment 3

In this experiment, optimal i_d for chosen fan volume Q was searched. Steps in experiment were as follows:

- For each value of Q , working point $(\omega, Q, \Delta s)$ was find with the use of C# application (see 4.1). Figure 10 illustrates this.
- Computation of needed torque T_m from equation 16.
- Procedure from experiment 1 was applied, so optimal current i_{wl} was found.

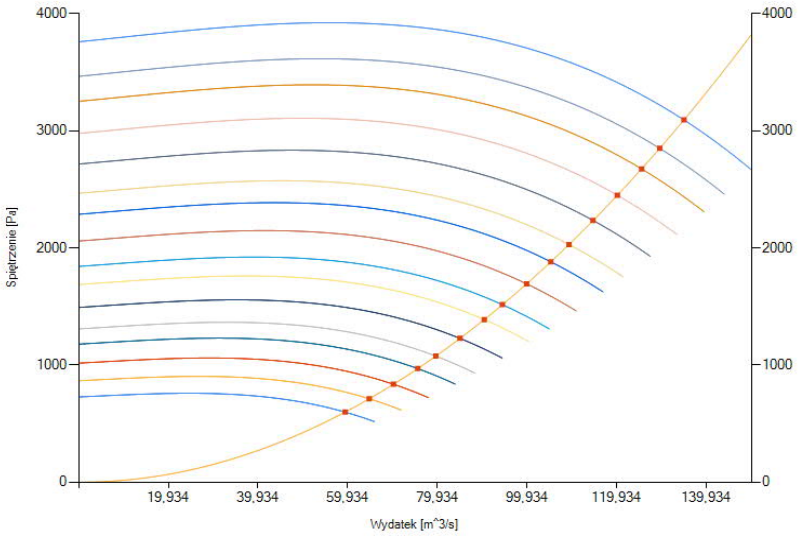

Fig. 10. Set of working points from range to

Tab. 1. Working points and optimal values of current i_{od}

$Q\left[m^3/s\right]$	$\frac{\omega}{\omega_N}$	$T_m[Nm]$	$i_{sd.opt}[A]$
135	1,001	2848	-27,1
130	0,964	2647	-26,0
125	0,927	2451	-24,9
120	0,890	2265	-23,8
115	0,853	2085	-22,6
110	0,816	1913	-21,4
105	0,779	1749	-20,2
100	0,741	1589	-18,9
95	0,704	1440	-17,6
90	0,667	1298	-16,2
85	0,630	1166	-15,0
80	0,593	1039	-13,7
75	0,556	921	-12,4
70	0,519	810	-11,2
65	0,482	707	-10,0
60	0,445	612	-8,7

5. Energy-efficient V/f Control

5.1. V/f control method for a PMSM without dumping windings

The V/f control method is proposed for a PMSM without dumping windings in the rotor. In this method the reference stator voltage is calculated in order to maintain a constant flux. This allows a nominal torque in the full range frequency to be obtained.

For the calculation of the magnitude of the voltage v_s the following equation was used:

$$v_S = i_S r_S \cos\varphi_{ui} + \sqrt{e_S^2 + (i_S r_S \cos\varphi_{ui})^2 - (i_S r_S)^2} \tag{17}$$

where:

φ_{ui} – the angle between voltage (vs) and current (is) vector

$e_S = \lambda_m \omega$ - electromotive force

λ_m – torque constant

ω_r – reference speed.

The current vector is obtained by measuring three phase currents in a fixed coordinate system $\alpha\beta$:

$$i_S = \sqrt{i_\alpha^2 + i_\beta^2} \tag{18}$$

where:

$$i_\alpha = \frac{1}{3}(2i_a - i_b - i_c) \tag{19}$$

$$i_\beta = \frac{1}{\sqrt{3}}(i_b - i_c) \tag{20}$$

The term $i_s\cos\varphi_{ui}$ is calculated from the equation:

$$i_s \cos\phi_{ui} = \frac{2}{3}\left[\begin{array}{l} i_a \cos\phi_u + i_b \cos\left(\phi_u - 120^o\right) + \\ + i_c \cos\left(\phi_u + 120^o\right) \end{array}\right] \tag{21}$$

where:

φ_u – voltage vector angle

i_a, i_b, i_c – motor phase currents.

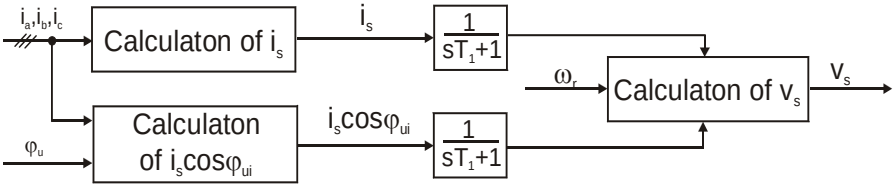

Fig 11. The algorithm for calculating the voltage v_s

In order to eliminate high frequency distortion in the current is a low pass filter was used. The algorithm for calculating the stator voltage vs is shown in Figure 11.

To stabilize the system for the full frequency range, additional damping of the rotor is required. This can be achieved by an appropriate modulation of the frequency of the motor [7]. The simplified dynamics model, presented in [13] is used for the analysis. This model allows the predicting of how the applied frequency should be modulated to add damping to the system with PMSM. In addition, the speed disturbance is the main cause of the power perturbations for an operating point. Based on this analysis, the applied frequency should be modulated as:

$$\Delta\omega_e = -k\Delta p_e \tag{22}$$

where Δp_e – perturbation of power for an operating point. This value can be expressed as an electrical power signal after passing through the high pass filter

$$\Delta p_e = \left(1 - \frac{1}{sT+1}\right) p_e = \left(\frac{sT}{sT+1}\right) p_e \tag{23}$$

where input power p_e of the PMSM is given by:

$$p_e = \frac{3}{2} v_s i_s \cos\phi_{ui} \tag{24}$$

The algorithm for calculating the frequency modulation signal $\Delta\omega_e$ is shown in Figure 12.

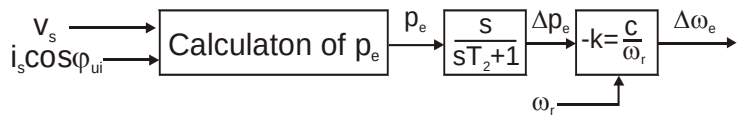

Fig 12. The algorithm for calculating the frequency modulation signal $\Delta\omega_e$

The block diagram of the open control system V/f with stabilizing loop is shown in Figure 13.

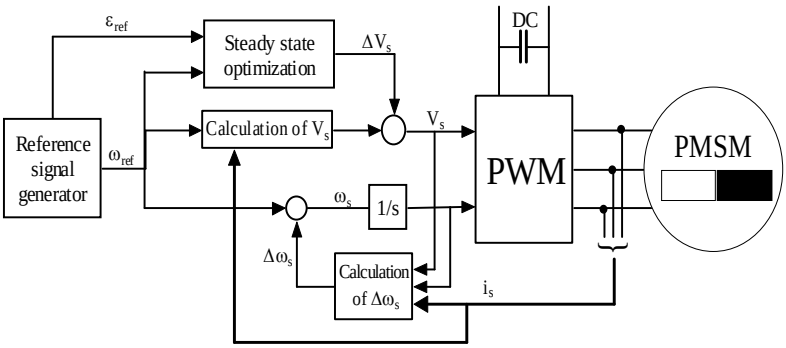

Fig 13. Structure of PMSM drive with stabilizing loop and steady state optimization

5.2. Tuning of stator voltage amplitude to energy-efficient working state

Optimization of the motor in steady state operation can be done in the on-line or off-line structure. The on-line method is based on the measurement of power losses, and uses a search algorithm to tune a control variable to achieve a minimum loss working condition. The optimizing controller does not depend on a loss model and is robust to variations in the motor parameters, such as temperature. Correct measurement of losses is unfortunately often difficult to implement in practice. The off-line method is based on a loss model of the machine. This approach can be used when the losses in the machine can be easily modeled in terms of input signals. This method can usually be easily implemented using look up table methods. This method is proposed in this paper.

In a permanent magnet motor with no core loss, a drive that operates at nearly zero d-axis current components will be optimally efficient. In steady state, the amplitude of the motor supply voltage influences the *d* component of the currents, while a *q*-axis current component is determined by the load torque.

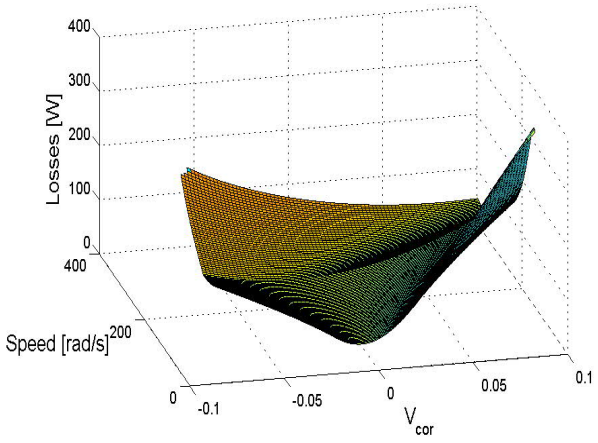

Fig 14. Power losses versus speed and correction voltage

With a fan drive there is an explicit dependence of load torque on the speed. After a series of simulations tests a steady state optimization table is created. The reference acceleration input is used to determine the steady state. The output signal is the fine-grained reference voltage correction. The optimization table is based on power losses in drive. The total power losses consist of winding losses and core losses. Are losses are calculated in detailed motor model. The results of optimization are shown on fig. 14. The power losses depend on

reference speed and applied voltage correction. The minimum value of power losses is search in the table.

5.3. Simulation Results

A motor simulation model was built in Matlab based on standard motor equations (1)-(6). For suitable modeling of the static torque, the static friction model with zero speed analysis [11] was used. A PWM inverter was modeled as an ideal P gain with additional delays. At the present stage of research it is assumed that the current measurement is ideal. The reference speed is generated by a reference signal generator with acceleration and jerk limits.

To demonstrate the effectiveness of the proposed method, some results of the simulation are presented. The test consists of three phases: startup, changing speed and braking. Figure 15 a) shows the waveforms for the system without the optimization block. The drive is working properly. Actual speed closely follows the reference speed. The frequency correction signal provides stable operation. The current component in the q-axis is related to the load torque. Unfortunately the d-axis current increases the losses in the drive. During the presented test the energy delivered to the motor was 7.11 kJ. The sum of losses in winding and losses in iron was equal 1.72 kJ.

Figure 15 b) shows the waveforms for the system with the optimization block. Under steady state conditions the d-axis current is reduced to almost zero. Also the reduction of the d-axis current is shown in the dynamic states. In this case the energy delivered to the motor was 6.69 kJ. The sum of losses in winding and losses in iron was equal 1.49 kJ. The efficiency of the drive has increased by about 2%.

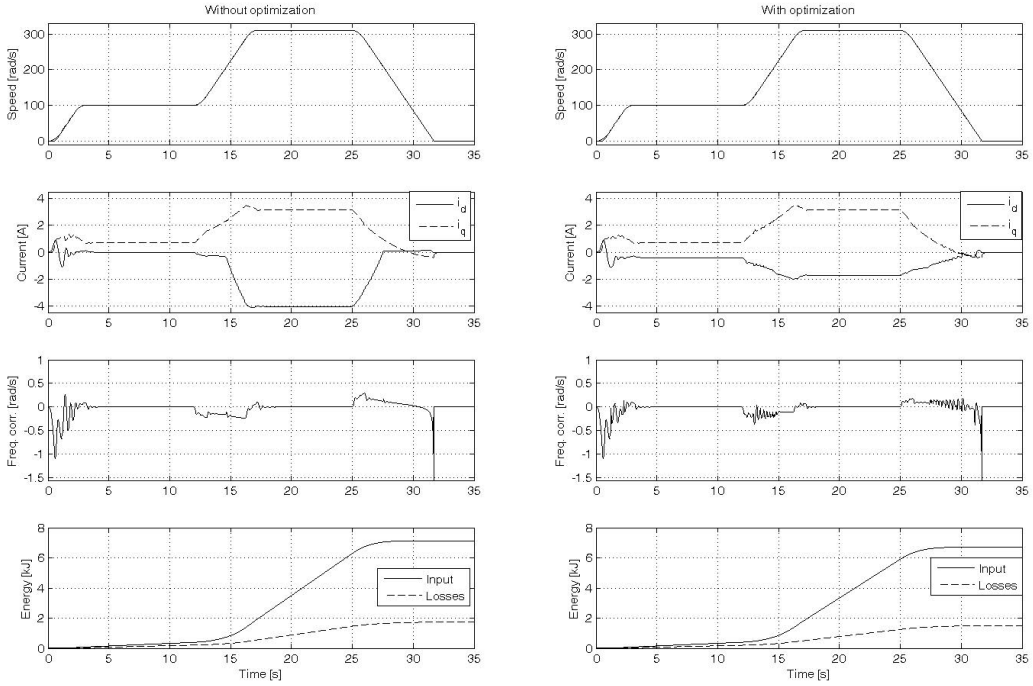

a) without optimization b) with optimization

Fig. 15. Simulation results for system without/with optimization block.

1 row: reference speed (dashed line) and drive speed (solid line); 2 row: i_q current (dashed line) and i_d current (solid line); 3 row: frequency correction;4. row: Input energy (solid line) and losses energy (dashed line).

6. Conclusion

The method of the PM motor control presented in this paper is suitable for applications requiring a low dynamic, like pumps and fans. This method does not use position sensors or position estimators. The off-line optimizing method is applied to achieve minimum power losses. The method presented will be implemented in a real industrial drive with low and middle sized fans.

Acknowledgment

This work was realized within the project "New generation of energy-saving electric drives for pumps and cooling fans in mining industry", agreement no. POIG.01.01.02-00-113/09, The Operational Programme Innovative Economy, financial perspective between 2007-2013.

References

1. P. Vas, *Sensorless vector and direct torque control* . Oxford University Press, 1998.
2. S. Brock, and J. Deskur, *The problem of measurement and control of speed in a drive with an inaccurate measuring position transducer* , 10th IEEE International Workshop on Advanced Motion Control, pp. 132-136, 26-28 March 2008.
3. T. Pajchrowski, and K. Zawirski, *Application of artificial neural network to robust speed control of servodrive* , IEEE Transaction on Industrial Electronics, vol. 54, no. 1, pp.200-207, February 2007.
4. Morimoto, K. Kawamoto, M. Sanada, and Y. Takeda, *Sensorless control strategy for salient-pole PMSM based on extended EMF in rotating reference frame* , IEEE Trans. Ind. Applicat., vol. 38, pp. 1054-1061, July/August 2002.
5. D. Janiszewski, *Extended Kalman filter based speed sensorless PMSM control with load reconstruction* , Vedran Cordic, Kalman Filter InTech, Vienna 2010.
6. S. Bolognani, L. Tubiana, and M. Zigliotto: *Extended Kalman filter tuning in sensorless PMSM drives*, IEEE Trans. Ind. Applicat., vol. 39, pp. 1741-1747, November/December 2003.
7. P.D. Chandana Perera, F. Blaabjerg, J.K. Pedersen, and P. Thogersen, *A sensorless, stable V/f control method for permanent-magnet synchronous motor drives* , IEEE Trans. Ind. Applicat., vol. 39, pp. 783-791, May/June 2003.
8. R.S. Colby, and D.W. Nowotny, *An efficiency-optimizing permanent magnet synchronous motor drive* , IEEE Trans. Ind. Applicat., vol. 24, pp. 462-469, May/June 1988.
9. Y. Nakamura, T. Kudo, F. Ishibashi, and S. Hibino, *High-efficiency drive due to power factor control of a permanent synchronous motor* , IEEE Trans. Power Electron., vol. 10, pp. 247-253, March 1995.
10. M. Kiuchi, T. Ohnishi, H. Hagiwara, and Y. Yasuda, *V/f control of permanent magnet synchronous motors suitable for home appliances by DC-link peak current control method*, International Power Electronic Conference, IPEC, pp. 567-573, 2010.

11. B. Armstrong-Hélouvry, P. Dupont, and C.C. De Wit, *A survey of models, analysis tools and compensation methods for the control of machines with friction* , Automatica, vol. 30, no. 7, pp. 1083–1138, 1994.

12. Brock S., Pajchrowski T. *Energy-optimal v/f control of permanent magnet synchronous motors for fan applications* Sympozjum Maszyn Eelektrycznych, Szczecin 2011

13. Brock S. *Badanie stabilności napędu wentylatora z silnikiem synchronicznym z magnesami trwałymi sterowanego w układzie otwartym.* Studia z Automatyki i Informatyki, tom 35, 2010 ss. 7 – 17

14. Cavallaro. C. at. el. *Analysis a DSP Implementation and Experimental Validation of a Loss Minimization Algorithm Applied to Permanent Magnet Synchronous Motor Drives.* Industrial Electronics Society, 2003. IECON '03. The 29th Annual Conference of the IEEE

15. Nowak L., Kowalski K., Stachowiak D., Mikołajewicz J., Pietrowski W., Radziuk K., *Wyznaczanie optymalnego punktu pracy i charakterystyki obciążenia silników synchronicznych do napędu wentylatorów.* XVI Conference Computer Applications in Electrical Engineering., Poznań, April 11-13, 2011

16. http://www.landys.com/en/index.html

17. Ślązak N., Borowski M., Obracaj D. Example of main ventilation reversion in a coal mine. Materiały Konferencyjne Szkoły Eksploatacji Podziemnej, 2005